EJN fens European Journal of Neuroscience

European Journal of Neuroscience, Vol. 39, pp. 688–702, 2014 doi:10.1111/ejn.12434

DISORDERS OF THE NERVOUS SYSTEM

Dysfunctional and compensatory synaptic plasticity in Parkinson's disease

Henning Schroll,[1,2,3,4] Julien Vitay[4] and Fred H. Hamker[1,4]
[1]Bernstein Center for Computational Neuroscience, Charité – Universitätsmedizin Berlin, Berlin, Germany
[2]Psychology, Humboldt Universität zu Berlin, Berlin, Germany
[3]Neurology, Charité – Universitätsmedizin Berlin, Berlin, Germany
[4]Computer Science, Chemnitz University of Technology, Straße der Nationen 62, Chemnitz, Germany

Keywords: basal ganglia, computational model, connectivity, learning, reward

Abstract

In Parkinson's disease, a loss of dopamine neurons causes severe motor impairments. These motor impairments have long been thought to result exclusively from immediate effects of dopamine loss on neuronal firing in basal ganglia, causing imbalances of basal ganglia pathways. However, motor impairments and pathway imbalances may also result from dysfunctional synaptic plasticity – a novel concept of how Parkinsonian symptoms evolve. Here we built a neuro-computational model that allows us to simulate the effects of dopamine loss on synaptic plasticity in basal ganglia. Our simulations confirm that dysfunctional synaptic plasticity can indeed explain the emergence of both motor impairments and pathway imbalances in Parkinson's disease, thus corroborating the novel concept. By predicting that dysfunctional plasticity results not only in reduced activation of desired responses, but also in their active inhibition, our simulations provide novel testable predictions. When simulating dopamine replacement therapy (which is a standard treatment in clinical practice), we observe a new balance of pathway outputs, rather than a simple restoration of non-Parkinsonian states. In addition, high doses of replacement are shown to result in overshooting motor activity, in line with empirical evidence. Finally, our simulations provide an explanation for the intensely debated paradox that focused basal ganglia lesions alleviate Parkinsonian symptoms, but do not impair performance in healthy animals. Overall, our simulations suggest that the effects of dopamine loss on synaptic plasticity play an essential role in the development of Parkinsonian symptoms, thus arguing for a re-conceptualisation of Parkinsonian pathophysiology.

Introduction

Motor symptoms in Parkinson's disease (PD) result from a loss of dopamine in the basal ganglia (BG). However, the mechanisms by which dopamine loss causes BG dysfunctions and ultimately hypokinesia are not yet well understood. An influential set of theories dating back to the late 1980s (Albin *et al.*, 1989; DeLong, 1990) proposes that motor decay originates from an imbalance of excitatory and inhibitory pathways in BG: the direct BG pathway (cortex→striatum→globus pallidus internus) which facilitates activity in motor cortex is assumed to become less active by dopamine loss, while the indirect pathway (cortex→striatum→globus pallidus externus→subthalamic nucleus→globus pallidus internus) which inhibits activity in motor cortex is assumed to become more active. These theories are widely accepted in their core proposals and have been corroborated by empirical evidence (Kravitz *et al.*, 2010). However, they do not explain some paradoxical effects of BG surgery (Marsden & Obeso, 1994): lesions of globus pallidus internus (GPi), a BG output structure, for example, substantially alleviate Parkinsonian motor symptoms (Vitek *et al.*, 2003), but do not significantly impair motor performance in healthy animals (Horak & Anderson, 1984). Moreover, these theories merely propose global changes in pathway outputs, thus neglecting synapse-specific effects, and do not account for compensatory mechanisms in Parkinsonian BG (cf. Bezard *et al.*, 1999).

In response to these theories' shortcomings, Mink (1996) suggested that pathway dysfunctions differentially affect selected and competing (i.e. unselected) motor programs rather than affecting all of them equivalently. Specifically, he proposed that a reduced output of the direct pathway results in a specific deficit in facilitating selected motor programs, while a reduced output of the indirect pathway causes a deficit in inhibiting competing motor programs. Recent empirical evidence, however, has challenged the latter assumption (Kravitz *et al.*, 2010). Nambu (2005) extended and refined Mink's (1996) ideas: he proposed that in Parkinsonian brains, the direct pathway reduces its facilitation of selected motor programs, while the hyperdirect pathway (cortex→subthalamic nucleus→GPi) and the indirect pathway increase their suppression of both selected and competing motor programs. Overall thereby, selected motor programs are excited to a smaller degree and for a shorter period of time, while the number of inhibited motor programs increases. While this theory accounts for a large body of

Correspondence: Professor Fred H. Hamker, [4]Department of Computer Science, as above.
E-mail: fred.hamker@informatik.tu-chemnitz.de

Received 17 May 2013, revised 24 October 2013, accepted 25 October 2013

neurophysiological evidence (e.g. Nambu *et al.*, 2000; Tachibana *et al.*, 2008; Nishibayashi *et al.*, 2011), it does not specify the mechanisms via which dopamine loss causes pathway dysfunctions.

Recently, it has been shown in slices of mice brains that dopamine loss profoundly disturbs synaptic plasticity in BG pathways (Shen *et al.*, 2008): it facilitates long-term depression (LTD) in D1 medium spiny neurons of the direct pathway, but favors long-term potentiation (LTP) in D2 medium spiny neurons of the indirect pathway. To investigate if such effects of dopamine loss on synaptic plasticity can indeed account for altered neuronal activity and motor performance in PD and explain core predictions of previous theories, we developed a neuro-computational model.

Materials and methods

Model architecture

Our model consists of a cortico-basalganglio-thalamic (CBGT) loop (Fig. 1A) that contains direct, indirect and hyperdirect BG pathways as well as a cortico-thalamic pathway (Nambu *et al.*, 2002; Haber, 2003). Thus, we model the functionally most relevant fiber tracts of BG, but do not include all known connections (cf. Braak & Del Tredici, 2008) to avoid overlap between pathways and to focus on their major potential functions. These pathways spread between visual and motor cortices, thereby bridging the gap from stimulus to response. Each modeled brain area and nucleus consists of a pre-specified number of artificial neurons (cf. Table 1) whose firing rates are determined based on the sums of glutamatergic (i.e. excitatory) and GABAergic (i.e. inhibitory) synaptic inputs as well as a baseline rate. The direct BG pathway and the cortico-thalamic pathway have net excitatory effects on motor cortex, while indirect and hyperdirect pathways have net inhibitory effects (Fig. 1B). For the indirect pathway, distinct routes have been proposed (Smith *et al.*, 1998) of which we included the short one that does not contain the subthalamic nucleus (STN) – in accordance with previous computational models (e.g. O'Reilly & Frank, 2006; Stocco *et al.*, 2010). Thus, we avoided overlap between indirect and hyperdirect pathways. In accordance with previous theories and computational models, we assume BG pathways to be entirely distinct before converging in GPi. Although this is probably a simplification (Lévesque & Parent, 2005), it provides solid ground for our analyses. We further assume that thalamic motor signals are, via striatum, relayed back to pallidum (cf. Fig. 1B). As suggested by Brown *et al.* (2004), thalamic feedback may solve a credit-assignment problem after incorrect responses: it informs BG pathways which response has just failed to elicit reward and thus enables specific suppression of this response. Lateral competition in GPi favors selection of just a single response in each trial.

We do not pre-specify synaptic connectivity patterns or connectivity strengths in CBGT pathways, but define the mechanisms through which connectivity self-organises via synaptic plasticity. Thus, pathways initially do not implement any function, but have to establish their functions by adapting their synaptic weights. In line with empirical findings (Gerfen *et al.*, 1990; Shen *et al.*, 2008), we assume synaptic plasticity to be a function of dopamine, presynaptic activity and postsynaptic activity. In pathways that are equipped with D1 dopamine receptors (i.e. direct and hyperdirect pathways),

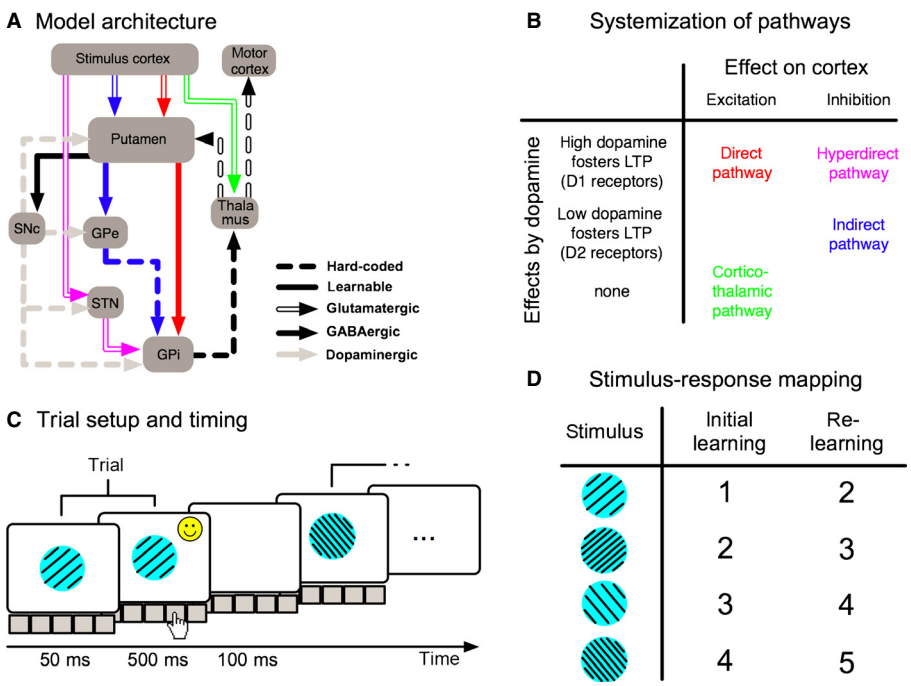

FIG. 1. Model architecture, systemisation of pathways and task. (A) Anatomical architecture of our neuro-computational model. Boxes denote anatomical structures, arrows the fibers between them. We implement only those pathways that are assumed to fulfill fundamental functions with respect to response selection, i.e. the direct BG pathway (cortex–putamen–GPi), the indirect BG pathway (cortex–putamen–GPe–GPi), the hyperdirect BG pathway (cortex–STN–GPi) and the cortico-thalamic pathway (cortex–thalamus). (B) Pathways are implemented to differ along two dimensions: they either excite or inhibit cortical activity and dopamine facilitates either LTP or LTD in their synapses (the latter effect being mediated by different types of dopamine receptors; cf. Boyson *et al.*, 1986; Gerfen *et al.*, 1990; Braak & Del Tredici, 2008; Shen *et al.*, 2008). (C) Trial set-up and timing of our stimulus-response task. Stimuli are presented to stimulus cortex; responses are read out of motor cortex. Fifty milliseconds after stimulus onset, one of five possible responses is selected based upon motor-cortex activity in the model. If the selection is correct, reinforcement is given immediately while the stimulus is still present. Trials are separated by inter-trial intervals of 100 ms. (D) Stimuli and rewarded responses. Four stimuli vary along two dimensions (illustrated as spatial frequency and orientation). For each stimulus, only one particular response (numbers 1–5) is rewarded if chosen. Correct (i.e. rewarded) responses change for the re-learning task phase.

TABLE 1. Numbers of cells for each of the model's layers as well as parameters and transfer functions for computing membrane potentials and firing rates

Cell type	No. of cells	$f_r(x) =$	w^{ff}	w^{ff}	w^{lat}	B	$\varepsilon_{i,t}$
Stimulus cortex	4	x				0.0	0.0
Motor cortex	5	x	$w_{i,j}^{\text{Thal}-\text{Cx}} = 1.0$		$w_{i,j}^{\text{Cx}-\text{Cx}} = -1.0$	0.0	[−1.0 1.0]
Striatum (D1)	16	x			$w_{i,j}^{\text{Str (D1)}-\text{Str (D1)}} = -0.3$	0.4	[−0.1 0.1]
Striatum (D2)	16	x			$w_{i,j}^{\text{Str (D2)}-\text{Str (D2)}} = -0.3$	0.4	[−0.1 0.1]
Striatum (Thal)	5	x	$w_{i,j}^{\text{Thal}-\text{Str(Thal)}} = 1.0$		$w_{i,j}^{\text{Str(Thal)}-\text{Str(Thal)}} = -0.3$	0.4	[−0.1 0.1]
STN	16	x			$w_{i,j}^{\text{STN}-\text{STN}} = -0.3$	0.4	[−0.1 0.1]
GPe	5	x	$w_{i,j}^{\text{Str(Thal)}-\text{GPe}} = -0.3$			1.0	[−1.0 1.0]
GPi	5	x	$w_{i,j}^{\text{GPe}-\text{GPi}} = -1.5$	$w_{i,j}^{\text{Str(Thal)}-\text{GPi}} = -0.3$		2.4	[−1.0 1.0]
Thalamus	5	$\begin{cases} x & \text{if } 0 \le x \le 1 \\ 0.5 + \frac{1}{1+e^{\frac{1-x}{2}}} & \text{else} \end{cases}$	$w_{i,j}^{\text{GPi}-\text{Thal}} = -1.5$		$w_{i,j}^{\text{Thal}-\text{Thal}} = -0.6$	1.0	[−0.1 0.1]
SNc	1	x				0.1	0.0

For each modeled brain area and nucleus, numbers of simulated neurons are given, as well as these neurons' firing-rate transfer functions ($f_r(x)$), hard-coded feed-forward weights (w^{ff}), lateral weights (w^{lat}), baseline membrane parameters (B) and uniform distributions from which random noise terms ($\varepsilon_{i,\ t}$) are drawn. GPe, globus pallidus external segment; GPi, globus pallidus internal segment; SNc, substantia nigra pars compacta; STN, subthalamic nucleus; striatum (Thal), striatal neurons that receive thalamic feedback.

high levels of dopamine facilitate LTP, while low levels facilitate LTD (Fig. 1B). In pathways that are equipped with D2 dopamine receptors (i.e. the indirect pathway), high and low levels exert exactly opposite effects. For illustration, Fig. 2 presents the effects of dopamine-receptor stimulation and dopamine-receptor blocking on D1-type and D2-type striatal medium spiny neurons (MSNs) in our model (cf. Shen *et al.*, 2008).

When we train the model on a stimulus–response (SR) reinforcement-learning task as described below, stimuli are fed into stimulus cortex and the model's responses are recorded from motor cortex. With a correct response, a reward signal is fed into the substantia nigra compacta (SNc) where a reward-prediction signal (of opposite sign) is added as specified in 'Mathematical set-up'. In line with empirical evidence (Hollerman & Schultz, 2003), SNc activity peaks above baseline whenever more reward is received than predicted; it dips below baseline in the case of unexpectedly little reward. SNc firing determines dopamine levels in BG nuclei and thereby modulates synaptic plasticity in BG pathways. To provide an insight into model dynamics, Fig. 3 shows how activity spreads through the different nuclei of a healthy, randomly initialised network that has already been trained on an SR task (cf. 'Behavioral task').

The model's parameters were determined such that it is capable of SR learning under normal dopamine levels; only afterwards did we simulate Parkinsonian dopamine loss and investigated how this causes CBGT pathway dysfunctions and behavioral impairments.

Mathematical set-up

The model contains a predefined number of rate-coded neurons for each of the modeled brain regions and nuclei (cf. Table 1). Differential equations control these neurons' membrane potentials and firing rates as well as synaptic plasticity between them. All differential

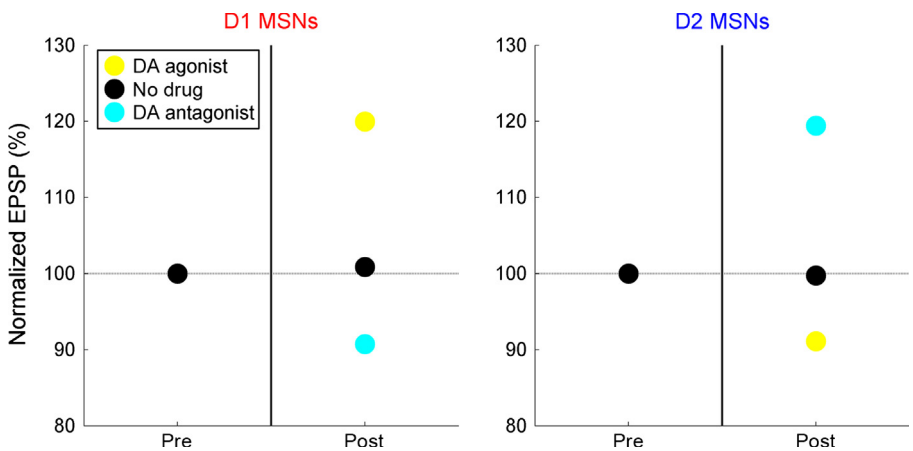

FIG. 2. Effects of dopamine agonists and antagonists on synaptic plasticity in D1- and D2-type striatal MSNs in our model. To measure the effects of synaptic plasticity, magnitudes of excitatory postsynaptic potentials (EPSPs) are measured both before (pre) and after (post) the induction of plasticity. EPSPs are elicited by setting presynaptic activity to a value of 1.0 for 50 ms and recording postsynaptic activity at the end of this period. Synaptic plasticity is induced by setting activity of a presynaptic (cortical) neuron to 1.0, activity of a postsynaptic (striatal) neuron to 0.5 and dopamine to either baseline (no drug), 0.1 points above baseline (dopamine agonist) or 0.1 points below baseline (dopamine antagonist) for 150 ms. All other neurons in cortex and striatum are set to activities of 0.0. Synaptic strengths are initialised with a value of 0.5. Simulations are performed 1000 times for precise estimation of all effects.

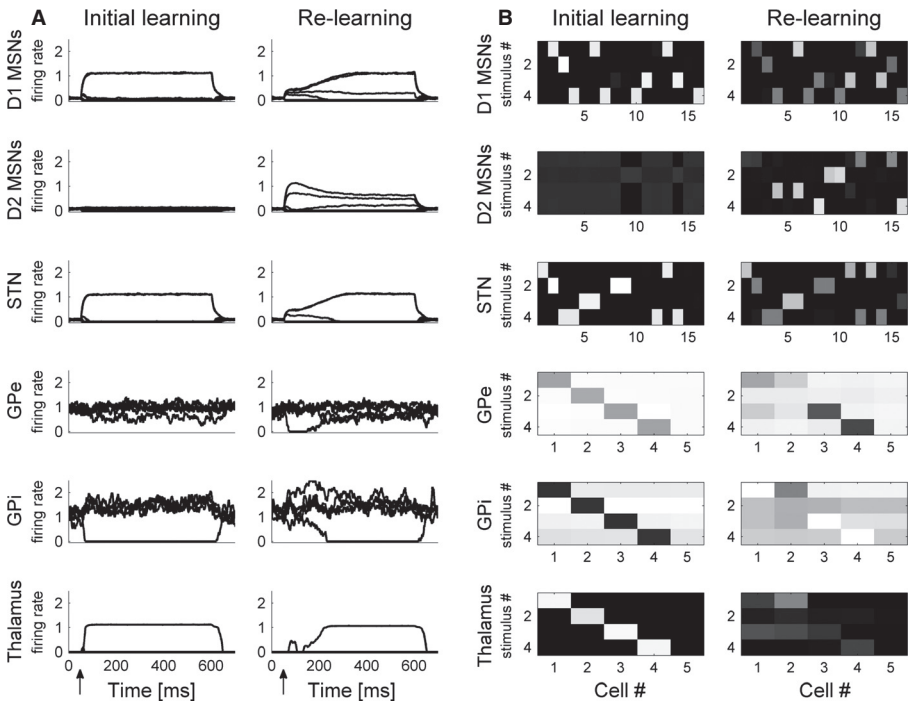

FIG. 3. Activities recorded from a healthy randomly initialised network performing our SR task. (A) Single-cell firing rates recorded from different nuclei during initial learning and re-learning. Lines depict firing rates of different neurons over the course of a single trial; arrows denote stimulus onset. When initial learning is just accomplished (left subplots), stimulus presentation activates some D1 MSNs that inhibit firing of a specific GPi neuron (corresponding to the correct motor program), while STN cells increase the activities of all other GPi neurons. In thalamus and motor cortex therefore, a specific motor program becomes activated, which results in a specific (correct) response. During re-learning (right subplots), stimulus presentation additionally activates some D2 MSNs of the indirect pathway that inhibit activity of a specific GPe neuron (encoding the previously correct motor program) such that the neuron's inhibition of a specific GPi neuron is reduced and the previously correct response is inhibited. (B) Firing rates of all individual neurons of BG and thalamus averaged over the last 50 trials of the initial-learning period and the first 75 trials of the re-learning period, separately for trials in which stimuli 1, 2, 3 and 4 were presented. Bright shadings denote high activities, while dark shadings denote low activities (where 'white' corresponds to firing rates of 1.5 for GPi cells and firing rates of 1.0 for all other cells and 'black' corresponds to firing rates of 0.0 for all cells). At the end of the initial-learning period (left subplots), each stimulus activates a different set of D1 MSNs (direct pathway) and STN cells (hyperdirect pathway), while D2 MSNs (indirect pathway) are not activated. D1 MSNs, via GPi, then activate those thalamic cells that correspond with correct motor programs (i.e. cell 1 for stimulus 1, cell 2 for stimulus 2, etc.), while STN cells suppress activities of all other thalamic cells. At the beginning of re-learning (right subplots), D2 MSNs (indirect pathway) get activated upon stimulus presentation. These D2 MSNs suppress activities of those thalamic cells (via GPe and GPi) that correspond to previously correct motor programs (note that these thalamic cells still receive some activation because of cortico-thalamic fibers). At the same time, D1 MSNs and STN cells start establishing new SR associations in line with novel reinforcement contingencies (stimulus 1, for instance, appears to be already linked to its correct response 2).

equations are integrated via the Euler method with a time-step of 1 ms (cf. Vitay & Hamker, 2010). Membrane potentials $m_{j,t}^{\text{post}}$ are computed via

$$\tau \cdot \frac{\mathrm{d}m_{i,t}^{\text{post}}}{\mathrm{d}t} + m_{i,t}^{\text{post}} = \sum_{j \in \text{pre}} \left(w_{i,\,j,t}^{\text{pre}-\text{post}} \cdot r_{j,t}^{\text{pre}} \right) + B + \varepsilon_{i,t}, \qquad (1)$$

where $\tau = 10$ ms is a time constant, $w_{i,\,j,t}^{\text{pre}-\text{post}}$ is the strength (i.e. weight) of the synapse between presynaptic cell j and postsynaptic cell i, $r_{j,t}^{\text{pre}}$ is the firing rate of presynaptic cell j, B is a baseline membrane potential and $\varepsilon_{i,t}$ is a random noise term drawn from a uniform distribution as specified in Table 1.

Equation (1) does not apply to dopaminergic SNc cells, whose membrane potentials are instead governed by

$$\tau \cdot \frac{\mathrm{d}m_{i,t}^{\text{post}}}{\mathrm{d}t} + m_{i,t}^{\text{post}} = P_t \cdot \left(R_t + Q_t \cdot \sum_{j \in \text{pre}} \left(w_{i,\,j,t}^{\text{pre}-\text{post}} \cdot r_{j,t}^{\text{pre}} \right) \right) + B. \quad (2)$$

Here, P_t is a timing-factor set to 1 whenever reward can potentially occur and to 0 otherwise, R_t is a reward term set to $(1-B)$ when reward is given and to 0 otherwise and Q_t is a scaling factor for reward prediction as explained below. Equation (2) determines that SNc activity increases above baseline rate B whenever there is more reward (R_t) than predicted and decreases below baseline whenever there is less reward than predicted (thus encoding reward prediction errors). The reward prediction at time t is encoded in the total amount of input from striatal D1 MSNs to SNc (i.e. in the sum of products of presynaptic striatal firing rates, $r_{j,t}^{\text{pre}}$, and synaptic strengths between striatum and SNc, $w_{i,j,t}^{\text{pre}-\text{post}}$). Strengths of synapses between D1 MSNs and SNc are learnable as specified in Table 2 such that reward predictions may be constantly updated: whenever SNc fires above baseline (because there is more reward than predicted), synapses between concurrently active presynaptic D1 MSNs and postsynaptic SNc cells become strengthened, thus resulting in a stronger reward prediction for the future. Whenever SNc fires below baseline rate (because there is less reward than predicted), by contrast, these connections experience LTD, resulting in a weakened reward prediction. The scaling factor Q_t is set to 1 in the case of reward and to 10 in the case of no reward; it thus strengthens small phasic decreases in SNc activity: in the initial stages of learning, reward predictions are not yet strong, so positive reward prediction errors are large, while negative reward prediction errors are small. Without Q_t, this imbalance would result in strong phasic increases in SNc activity, but only small phasic decreases,

TABLE 2. Parameters and transfer functions for computing synaptic plasticity

Connection	$f_{DA}(x)$ =	$f_{pre}(x)$ =	$f_{post}(x)$ =	$f_{\alpha}(x)$ =	η	η^{dec}	γ^{pre}	γ^{post}	m^{MAX}	CT
Cortex–striatum (D1)	$\begin{cases} 2x & \text{if } x>0 \\ 0.8x & \text{if } x<0 \cap \left(\begin{matrix} (Ca_{i,j,t}^{Cx-Str\,(D1)}>0 \cap w_{i,j,t}^{Cx-Str\,(D1)}>0) \cup \\ (Ca_{i,j,t}^{Cx-Str\,(D1)}<0 \cap w_{i,j,t}^{Cx-Str\,(D1)}<0) \end{matrix} \right) \\ 0 & \text{else.} \end{cases}$	x	x^+	x^+	75	250	0.15	0	1	1
Cortex–striatum (D2)	$\begin{cases} -2x & \text{if } x<0 \\ -0.8x & \text{if } x>0 \cap \left(\begin{matrix} (Ca_{i,j,t}^{Cx-Str\,(D2)}>0 \cap w_{i,j,t}^{Cx-Str\,(D2)}>0) \cup \\ (Ca_{i,j,t}^{Cx-Str\,(D2)}<0 \cap w_{i,j,t}^{Cx-Str\,(D2)}<0) \end{matrix} \right) \\ 0 & \text{else.} \end{cases}$	x	x^+	x^+	75	250	0.15	0	1	1
Cortex–STN	$\begin{cases} 2x & \text{if } x>0 \\ 0.8x & \text{if } x<0 \cap \left(\begin{matrix} (Ca_{i,j,t}^{Cx-STN}>0 \cap w_{i,j,t}^{Cx-STN}>0) \cup \\ (Ca_{i,j,t}^{Cx-STN}<0 \cap w_{i,j,t}^{Cx-STN}<0) \end{matrix} \right) \\ 0 & \text{else.} \end{cases}$	x	x^+	x^+	75	250	0.15	0	1	1
Striatum (D1)–GPi	$\begin{cases} 2x & \text{if } x>0 \\ 0.8x & \text{if } x<0 \cap Ca_{i,j,t}^{Str-GPi}>0 \\ 0 & \text{else.} \end{cases}$	x^+	$-x$	$-(-x)^+$	50	250	0	−0.15	−1	−1
STN–GPi	$\begin{cases} 2x & \text{if } x>0 \\ 0.8x & \text{if } x<0 \cap Ca_{i,j,t}^{STN-GPi}>0 \\ 0 & \text{else.} \end{cases}$	x^+	x	x^+	50	250	0	−0.15	1.5	1
Striatum (D2)–GPe	$\begin{cases} -2x & \text{if } x<0 \\ -0.8x & \text{if } x>0 \cap Ca_{i,j,t}^{Str-GPe}>0 \\ 0 & \text{else.} \end{cases}$	x^+	$-x$	$-(-x)^+$	50	250	0	−0.15	−2	−1
GPi–GPi	1	$(-x)^+$	$(-x)^+/x^{+*}$	x^+	1	1	0	0	0	1
Cortex–thalamus	1	x	x^+	x^+	2k	1	0	0.75	0.9	1
Striatum (D1)–SNc	$\begin{cases} x & \text{if } x>0 \\ 3x & \text{else.} \end{cases}$	x^+	1	0	100k	1	0	0	0	−1

For each plastic fiber tract in our model, the parameters that determine synaptic plasticity are given. We report transfer functions for dopamine factors of our learning rules ($f_{DA}(x)$), presynaptic factors ($f_{pre}(x)$), postsynaptic factors ($f_{post}(x)$) and α ($f_{\alpha}(x)$) for each of the model's fiber tracts. Further, time constants (η and η^{dec}), threshold parameters of pre- and postsynaptic factors (γ^{pre} and γ^{post}) and parameters controlling maximal desired membrane potentials (m^{MAX}) are given. Cortex here signifies stimulus cortex. GPe, globus pallidus external segment; GPi, globus pallidus internal segment; SNc, substantia nigra pars compacta; STN, subthalamic nucleus.
*For this connection, calcium traces contain different transfer functions for minuend and subtrahend of Eqn 4, as specified in 'Mathematical set-up'.

which would cause a tendency towards LTP in direct and hyperdirect pathways, and towards LTD in the indirect pathway. Because of this, random SR associations (that are routinely tried out during learning) would be established, but could not be dismissed if it turns out that they do not result in reward. Q_t now ensures relatively large decreases in SNc activity even for small negative reward prediction errors, which is in exact accordance with empirical findings (Bayer & Glimcher, 2005).

Firing rates $r_{i,t}^{post}$ are derived from membrane potentials via

$$r_{i,t}^{post} = f_r\left((m_{i,t}^{post})^+\right), \tag{3}$$

where $()^+$ defines that negative values are set to zero. Transfer functions $f_r(x)$ are layer-specific as detailed in Table 1. The layers' different firing rates, as depicted in Fig. 3A, were chosen to comply with the nuclei's different levels of tonic activity (cf. Nambu *et al.*, 2000; Kita & Kita, 2011).

Plasticity of cortico-thalamic synapses and of lateral synapses within GPi is guided by two-factor Hebbian-like learning rules (i.e. it depends upon pre- and postsynaptic activities only). Plasticity of all other synapses, by contrast, follows three-factor learning rules (i.e. it depends upon presynaptic activities, postsynaptic activities and dopamine). In this more general three-factor case, learnable weights $w_{i,j,t}^{pre-post}$ are computed via

$$\eta \cdot \frac{dw_{i,j,t}^{pre-post}}{dt} = CT \cdot f_{DA}(DA_t - B_{DA}) \cdot Ca_{i,j,t}^{pre-post} - \alpha_{i,t}^{post} \cdot Ca_{i,j,t}^{pre-post} \tag{4}$$

with

$$\alpha_{i,t}^{post} = f_{\alpha}\left(m_{i,t}^{post} - m^{MAX}\right). \tag{5}$$

Here, η is a time constant as specified in Table 2, $f_{DA}(x)$ a transfer function, DA_t the dopamine level at time t, $B_{DA} = 0.1$ the baseline dopamine level (which is kept constant across medical conditions and thus differs from the tonic dopamine level when simulating PD) and $Ca_{i,j,t}^{pre-post}$ a postsynaptic calcium level depending on pre- and post-

synaptic activities as defined in Eqn 6. CT defines the connection type and is set to 1 for glutamatergic (i.e. excitatory) and to −1 for GABAergic (i.e. inhibitory) synapses. Glutamatergic weights are prevented from decreasing below zero; GABAergic weights are prevented from increasing above it. For cortico-striatal and cortico-subthalamic fibers, as a special case, we allow synaptic strengths to take both positive and negative values to mimic the potential function of interneurons. $\alpha_{i,t}^{\text{post}}$ prevents connection strengths from increasing infinitely: it increases whenever postsynaptic membrane potentials increase above (or decrease below) a threshold defined by m^{MAX}.

Postsynaptic calcium levels $\text{Ca}_{i,j,t}^{\text{pre-post}}$ are computed via

$$\eta^{\text{Ca}} \cdot \frac{\text{d}Ca_{i,j,t}^{\text{pre-post}}}{\text{d}t} + \text{Ca}_{i,j,t}^{\text{pre-post}} = f_{\text{pre}}(r_{j,t}^{\text{pre}} - \overline{\text{pre}_t} - \gamma^{\text{pre}}) \cdot f_{\text{post}}(r_{i,t}^{\text{post}} - \overline{\text{post}_t} - \gamma^{\text{post}}) \quad (6)$$

with

$$\eta^{\text{Ca}} = \begin{cases} \eta^{\text{dec}} & \text{if } \eta^{\text{Ca}} \cdot \frac{\text{d}Ca_{i,j,t}^{\text{pre-post}}}{\text{d}t} + \text{Ca}_{i,j,t}^{\text{pre-post}} = 0 \\ 1 & \text{else.} \end{cases} \quad (7)$$

Here, $\overline{\text{pre}_t}$ and $\overline{\text{post}_t}$ are the mean activities of layers *pre* and *post* at time t and γ_{pre} and γ_{post} are threshold parameters. In brief, calcium levels increase for synapses where pre- and postsynaptic cells are concurrently active and decrease for all other synapses (cf. Schroll *et al.*, 2012). Transfer functions $f_{\text{pre}}(x)$ and $f_{\text{post}}(x)$ are given in Table 2. Equation 7 determines a gradual decay of calcium in the absence of concurrent pre- and postsynaptic activities. Table 2 shows, for each plastic fiber tract in our model, the parameters that determine synaptic plasticity.

Overt responses are defined probabilistically based upon motor-cortex firing rates via a soft-max rule. Probability of response i at time t, $P_{i,t}$, is given by

$$P_{i,t} = \frac{r_{i,t} + \theta}{\sum_{j \in \text{motor cortex}} (r_{j,t} + \theta)}. \quad (8)$$

$\theta = 10^{-10}$ prevents the denominator from becoming zero.

Random initialisations of networks apply to noise terms in Eqn 1, drawn from uniform distributions as specified in Table 1. All learnable synaptic connections are initialised with strengths of zero.

Behavioral task

For our simulation studies, we trained our model on an SR task and investigated its performance during initial learning, automatic execution and re-learning of this task. In each trial of the task, one of four stimuli was randomly chosen and presented (Fig. 1C). Each stimulus was assumed to consist of two features (e.g. orientation and spatial frequency), therefore being represented in the stimulus cortex of our model by simultaneous activation of two (out of four) cells. Fifty milliseconds after stimulus onset, the model's response was recorded from motor cortex via a softmax rule as specified in 'Mathematical set-up' and positive reinforcement was given in the case of a correct response. In the re-learning task phase, reinforcement contingencies were changed (Fig. 1D). We defined that a network had learned a given set of SR associations when it had reached a criterion of 50 correct responses in a row. When initial learning was mastered, we either specified that the network continued with the same set of rewarded SR associations (automatic-performance task phase) or we enforced a new set of rewarded SR associations by changing reward contingencies (re-learning phase). Networks that did not reach the initial-learning criterion within 5000 trials or both initial-learning and re-learning criteria within a total of 10 000 trials were abandoned and classified as failures.

Dopamine loss and dopamine replacement

To model Parkinsonian dopamine loss, we multiplicatively lowered SNc dopamine output to striatum and GPi. This resulted in decreases of both tonic and phasic dopamine levels. Nigro-striatal dopamine was lowered by 70%, nigro-pallidal dopamine by 40%. This asymmetry is in accordance with evidence that striatal dopamine decays faster than pallidal dopamine (Parent *et al.*, 1990; Whone *et al.*, 2003) and with findings that Parkinsonian symptoms do not arise before striatal dopamine depletion is well advanced (Moore, 2003). STN might not significantly lose its supply at all (Pavese *et al.*, 2011).

Dopamine replacement therapy (i.e. delivery of levodopa or dopamine agonists) is a standard treatment to alleviate Parkinsonian symptoms in humans. In the model, we implemented it by adding constant additional dopamine inputs to all BG nuclei, thus increasing tonic but not phasic levels. As dopamine replacement is delivered systemically in clinical practice (i.e. orally or via infusions), we defined that all BG nuclei received the same absolute amount of dopamine. We tested several dopamine doses to find out how dosage affects performance on our SR task (ranging from 12.5% to 200% of pallidal loss, in steps of 12.5%). To test the doses' effects on automatic performance, we first trained networks on our SR task and then simultaneously rendered them Parkinsonian and added dopamine replacement while task performance continued. To test replacement effects on initial-learning performance, we inflicted dopamine loss and granted replacement directly before we started the task.

BG lesions

For both healthy and Parkinsonian networks, we investigated behavioral outcomes of circumscribed lesions of striatum, STN, GPe and GPi. Technically, we forced all output of a lesioned nucleus to zero, i.e. damaged all of its neurons. To evaluate lesion effects on initial-learning performance, we inflicted lesions (and dopamine loss, if applicable) directly before the model was trained. To evaluate effects upon re-learning performance, we first trained unlesioned networks on the initial-learning phase of our task and then simultaneously inflicted lesions (and dopamine loss, if applicable) and started the re-learning phase. To evaluate effects upon automatic performance, we also trained unlesioned networks on the initial-learning phase first, then inflicted dopamine loss if applicable and finally, after an additional delay of 500 trials, inflicted the desired lesion. We recorded overt responses for a total of 2500 trials when measuring learning performances and for 25 000 trials when measuring automatic performance.

Analyses of pathway functions and dysfunctions

To investigate pathway functions and dysfunctions, we ran 1000 randomly initialised networks on our SR task for each medical condition, thus precisely estimating medians and quartiles of performance distributions and superseding statistical tests. From each network, we recorded overt responses, neuronal firing rates and synaptic strengths. During initial learning and re-learning, these data were recorded for each single trial, always 50 ms after stimulus onset (i.e. at the time of response selection). During automatic performance, these data were recorded only once in every ten trials to

limit file sizes (as automatic-performance simulations were run for 25 000 trials).

To determine the average output of a fiber tract, as depicted in Fig. 5, we first computed the product of each synapse's strength and its respective presynaptic activity during a particular task phase; afterwards, we averaged across all synapses. Effect sizes (ES) of average outputs, as depicted in Fig. 5, were then computed via

$$\mathrm{ES} = \frac{(\mathrm{mean(PD)} - \mathrm{mean(healthy)})}{\sqrt{(0.5 \cdot (\mathrm{var(PD)} + \mathrm{var(healthy)}))}}.$$

To determine a pathway's output on specific GPi cells, i.e. those that encode either correct or incorrect motor programs (as depicted in Figs 4, 7 and 8), we again computed products of synaptic strengths and presynaptic activities, but averaged only across those synapses that belong to the respective GPi cells (rather than across all synapses).

To plot developments of pathway outputs, we first binned each network's data and only afterwards computed statistics over networks, so as to cope with the networks' different learning speeds. Binning was done as follows: for each simulated network, we counted the number of trials n that were needed to perform a particular task phase. Then, we constructed 50 bins of which the first one contained all data from trials 1 to $n/50$ (rounded up), the second all data from trials $n/50 + 1$ to $2n/50$ and so on. Finally, we computed medians and quartiles for corresponding bins over all networks (i.e. separately for the first bin over all networks, for the second bin over all networks, and so on).

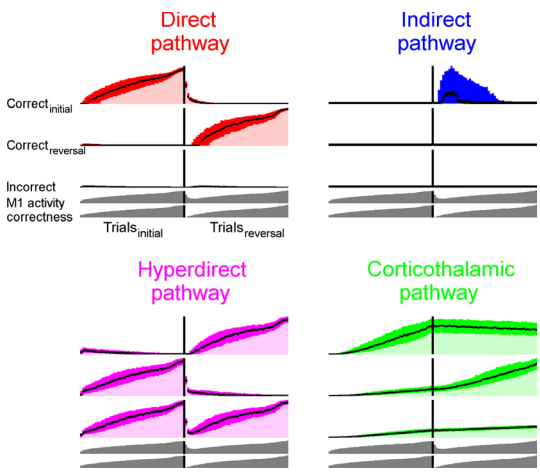

FIG. 4. Pathway outputs evolve over learning in healthy networks. Subplots depict how the outputs of the four major pathways develop along progress of initial learning and re-learning. Separate lines within each subplot show the evolution of pathway outputs on specific motor programs, namely those that are correct during initial learning (correct initial), during re-learning (correct reversal) or always incorrect. For each line, a brightly colored band depicts how lower and upper quartiles of pathway outputs (y axis) evolve over task progress (x axis) – as estimated from 1000 randomly initialised networks; a black line in each band visualises the development of the median. Pathway outputs are defined as the products of synaptic strengths and presynaptic activities, averaged across those synapses of each pathway that contribute to correct or incorrect responses, as detailed in 'Materials and methods'. For comparisons, developments of motor-cortical (M1) activities and correct-response rates are rendered below the developments of pathway outputs, where high y values indicate high M1 activity and high correct-response rates, respectively. Because of variability in the networks' learning performances, data were binned with regard to task progress as detailed in 'Materials and methods'.

Results

Pathway functions in healthy networks

To investigate how pathway functions evolve under normal dopamine levels, we ran 1000 randomly initialised networks on our SR task. Based on these data, we find the following pathway functions (Fig. 4): the direct pathway, in line with its generally acknowledged Go function (Brown *et al.*, 2004; O'Reilly & Frank, 2006; Vitay & Hamker, 2010), learns to facilitate correct motor programs (i.e. those that encode rewarded responses). When reward contingencies change, this pathway reduces its previous synaptic strengths and instead learns to facilitate the newly correct motor programs. The hyperdirect pathway learns to inhibit incorrect (i.e. currently unrewarded) motor programs that compete for execution with the correct ones; during re-learning it also readapts completely. This finding is in line with the assumption that the hyperdirect pathway performs a surround-inhibition of incorrect motor programs (Nambu *et al.*, 2002). The cortico-thalamic pathway learns to facilitate correct motor programs, just like the direct pathway. However, plasticity within the cortico-thalamic pathway is not modulated by dopamine. Thus, it does not directly learn from rewards. Rather, it learns to interconnect those cortical and thalamic neurons that are simultaneously activated via reward-sensitive BG pathways. The cortico-thalamic pathway develops more slowly than the direct BG pathway, but once established provides shorter and thus faster links between stimulus cortex and motor cortex (cf. Ashby *et al.*, 2007). When reward contingencies change, it does not immediately unlearn previously correct SR associations (which might become relevant again in the future), but rather maintains a synaptic memory of these associations. Our model predicts that, because of the cortico-thalamic pathway, BG are not required to perform well-learned SR associations; as shown in the lower left subplot of Fig. 9, GPi lesions (which totally eliminate BG output in our model) do not impair behavioral performance of well-learned tasks. However, if a conflict in automatic responding arises (i.e. when cortico-thalamic fibers facilitate two or more motor programs simultaneously), BG facilitation of the correct motor program remains necessary for its execution. Thus, our model reconciles two known functions of BG: we find them necessary both for SR learning via rewards (Seger, 2006) and for flexible performance of previously learned SR tasks under response conflict (cf. Redgrave *et al.*, 1999; McHaffie *et al.*, 2005; Leber *et al.*, 2008). The indirect BG pathway, finally, learns to inhibit previously correct motor programs when reward contingencies change (i.e. during re-learning). Such a function is in line with the indirect pathway's hypothesised NoGo function that is supposed to be triggered by negative reward prediction errors (Frank *et al.*, 2004; Frank, 2005; O'Reilly & Frank, 2006) and agrees with evidence on its role in reversal learning (Lee *et al.*, 2007; Jocham *et al.*, 2009). The indirect pathway does not get involved in inhibiting motor programs outside the context of re-learning; its function thus remains distinct from the hyperdirect pathway's function.

Average pathway outputs are altered in Parkinsonian networks

Early theories of Parkinsonian pathway dysfunctions propose that the direct BG pathway becomes less active in Parkinsonian networks, while the indirect pathway gets activated more strongly (Albin *et al.*, 1989; DeLong, 1990); and indeed, these assumptions have been corroborated by empirical evidence (Kravitz *et al.*, 2010). Our model allows us to investigate to what extent these activity changes of direct and indirect pathways can be accounted for by dysfunctional synaptic plasticity as resulting from dopamine loss.

Parkinson's disease typically develops relatively late in life, when all basic motor programs are already established. To mimic this in our simulations, we first trained our networks on our SR task and only afterwards inflicted dopamine loss by lowering SNc dopamine output to BG nuclei. As dopamine-lesioned networks continued to perform the previously learned task, we recorded average pathway outputs and average neuronal activities.

Our simulations corroborate the assumptions of the above-stated theories with regard to both direct and indirect pathways (Fig. 5): we indeed see a reduced average output of the direct pathway in Parkinsonian networks, while the indirect pathway increases its average output. These effects can thus be fully accounted for by dysfunctional synaptic plasticity. As another key assumption of the above-stated theories (Albin *et al.*, 1989; DeLong, 1990), the imbalance of direct and indirect pathways results in an increase in GPi firing and in subsequently reduced activities of thalamus and motor cortex. Our simulations again reproduce these effects: in unmedicated Parkinsonian networks, we find GPi activity increased by an effect size of 4.82 beyond what we record in healthy networks, while activities of thalamus and motor cortex are decreased by effect sizes of −0.49 and −2.00, respectively (Fig. 5). Surmounting the scope of the above-stated theories (Albin *et al.*, 1989; DeLong, 1990), our simulations predict that the average outputs of both hyperdirect and cortico-thalamic pathways are increased in Parkinsonian networks.

Dopamine replacement (i.e. systemic delivery of levodopa or dopamine agonists) is a standard treatment to reduce Parkinsonian symptoms. It has been shown to improve automatic SR performance in humans (Brown *et al.*, 1993) but to worsen learning of new SR associations (Jahanshahi *et al.*, 2010). Ameliorative vs. adverse effects depend upon replacement dosage. To simulate systemic dopamine replacement, we additively increased dopamine levels by equivalent absolute amounts in all BG nuclei. While this does not compensate for the diminution of phasic dopamine signals, it does increase tonic dopamine levels. To find a suitable dopamine dose, we systematically simulated different doses while running the automatic-performance and initial-learning phases of our task. We find that initial-learning performance is maximally alleviated by relatively low dopamine doses, while automatic performance requires relatively high doses to be restored (Fig. 6). Such high doses, however, impair learning. We investigated the reasons for these impairments in networks that received a replacement dose amounting to 187.5% of pallidal loss. As depicted in Fig. 6, learning performance was around chance level (i.e. 20% correct responses) for this dose of dopamine replacement. In 1000 randomly initialised networks, we investigated the types of errors that result in such poor performance. We observed that, on average, 99.69% of each network's responses (spanning trials 1–5000) could be explained by a single set of SR associations. This means that networks quickly converged on a set of (random) SR associations and then continued with these associations, although their responses did not result in reward. Such a development of random SR associations corresponds well with empirical reports that delivery of dopamine replacement often causes hyperkinetic symptoms in human patients (i.e. dyskinetic and/or choreic movements; Sporer, 1991; Rascol *et al.*, 2000). These symptoms can be thought of as inappropriate and highly repetitive motor responses in situations where in fact different responses or no response would be appropriate. Thus, our model not only explains ameliorative effects of dopamine medication, but also adverse effects that involve learning impairments and emergence of inappropriate 'hyperkinetic' SR associations.

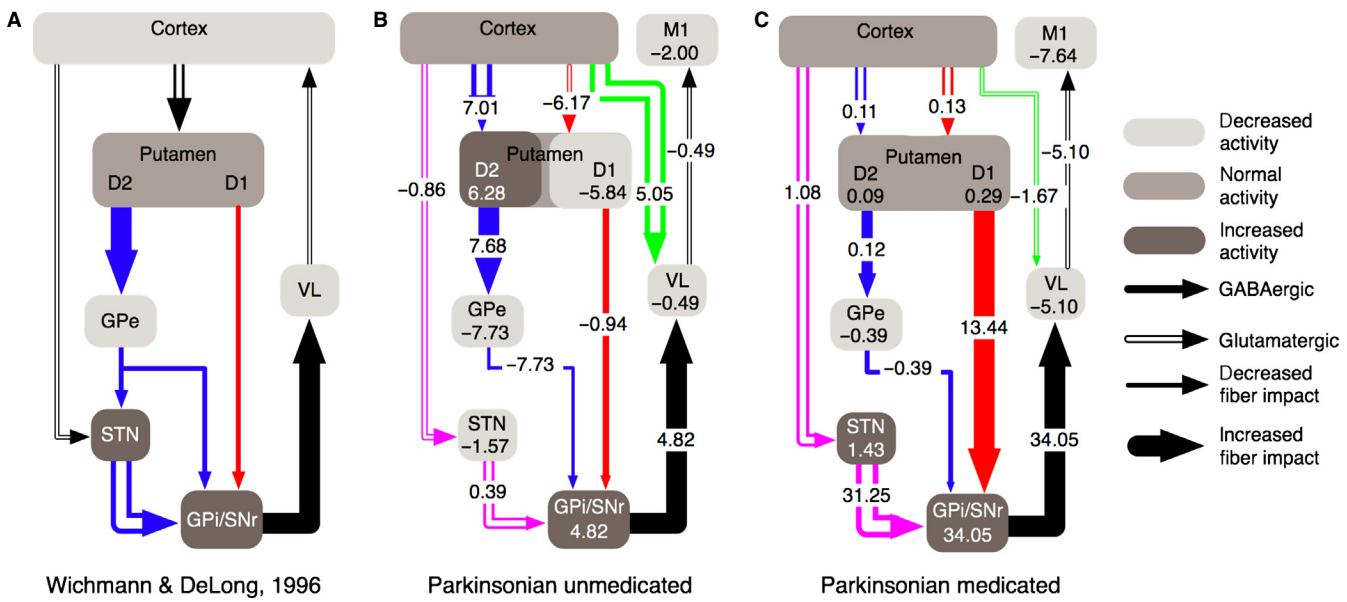

FIG. 5. Average pathway outputs and firing rates in Parkinsonian networks. (A) Core assumptions of the theories by Albin *et al.* (1989) and DeLong (1990) as summarised by Wichmann & DeLong (1996). Thin arrows denote reduced pathway outputs, thick arrows increased ones. Light gray shades denote decreased firing rates, dark gray shades increased firing rates. The output of the direct BG pathway is reduced, while the output of the indirect pathway is increased. Figure 5A is reprinted, with minimal adaptations, from Wichman & DeLong (1996). (B and C) Simulation results for Parkinsonian networks on and off medication. Numbers quantify differences between Parkinsonian and healthy networks in terms of effect sizes: numbers on top of arrows refer to effect sizes of average pathway outputs, numbers on top of nuclei to effect sizes of average firing rates. Average outputs are defined as the mean products of synaptic strengths and presynaptic activities, as detailed in 'Materials and methods'. For BG pathways therefore, the fiber tracts that point directly to GPi show the pathways' overall outputs (and contain all effects of cortical outputs to striatum and STN). Note that the indirect pathway in our model consists only of the direct link from GPe to GPi and does not contain the additional route via STN. Average pathway outputs and firing rates are computed over an interval of 10 000 trials, starting 15 000 trials after the beginning of dopamine loss. Effect sizes are computed as detailed in 'Materials and methods'.

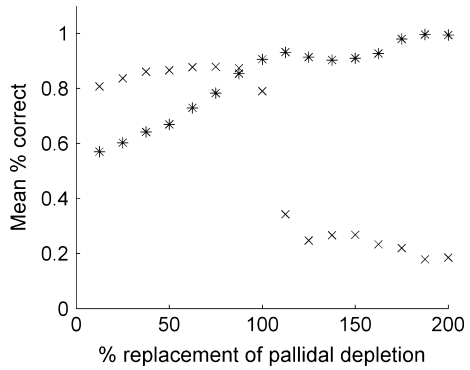

FIG. 6. Effects of dopamine replacement on behavioral performance in Parkinsonian networks. Average correct-response rates in both the automatic-performance phase (asterisks) and the initial-learning phase (crosses) of our task are shown for several simulated dopamine doses. While automatic performance requires relatively high doses of dopamine to be restored, learning performance drops with higher dopamine doses. For each simulated dose and task phase, 100 randomly initialised networks are run. Replacement doses are reported relative to the amount of dopamine loss in the pallidum (which differs from the amount of striatal dopamine loss as detailed in 'Materials and methods').

Such doses of dopamine replacement as are used in clinical practice have been shown to reduce symptoms in well-trained tasks but to impair learning performance (Brown *et al.*, 1993; Jahanshahi *et al.*, 2010). These effects correspond to relatively high doses of dopamine replacement in our model. Therefore, we used a relatively high dopamine dose amounting to 187.5% of pallidal loss for our simulations of pathway outputs (cf. Fig. 6). We find that such a dose restores the average outputs of indirect and cortico-thalamic pathways towards what we record in healthy networks (Fig. 5). However, it greatly enhances average outputs of direct and hyperdirect pathways, far beyond what we record in healthy networks (effect sizes are 13.44 and 31.25, respectively). These results argue against a merely restorative role of dopamine replacement, but rather suggest that replacement establishes a new equilibrium of average pathway outputs. The effects of dopamine treatment on pathway outputs have not yet received much attention by empiricists; we hope that our report motivates empiricists to scrutinise the predicted effects.

Pathway outputs on correct and incorrect motor programs are altered differentially in Parkinsonian networks

Our simulations allow us to investigate how far dysfunctional synaptic plasticity, as caused by dopamine loss, can account for differential changes in pathway outputs on correct and incorrect motor programs (Fig. 7). Mink (1996) and Nambu (2005) have stressed the importance of understanding such changes for comprehending the causes of PD symptoms. Based on our simulations, we find that the direct pathway's facilitation of *correct* motor programs decays in Parkinsonian networks (Fig. 7). This is in line with empirical evidence: dopamine lesions in rats eliminate phasic decreases in GPi firing that usually follow cortical stimulation in intact brain hemispheres (Kita & Kita, 2011) – in intact brains, these phasic decreases have been shown to be caused by the direct pathway and have been linked to a selection of appropriate actions (Nambu *et al.*, 2000). For the indirect pathway, we observe an increased inhibitory output on correct motor programs (Fig. 7). This is in line with findings that dopamine lesions in rats result in an increased phasic inhibition of GPe upon cortical stimulation, caused by the indirect pathway (Kita & Kita, 2011); however, it is not yet clear if this inhibition is indeed linked to a suppression of incorrect responses. For the hyperdirect pathway, we observe an increased inhibitory output on incorrect motor programs, primarily (but not exclusively) before behavioral impairments begin. Indeed, it has been shown that STN is hyperactive in presymptomatic Parkinsonian monkeys (Bezard *et al.*, 1999); moreover, dopamine loss in rats has been shown to result in an increased response of the hyperdirect pathway upon cortical stimulation (Kita & Kita, 2011) – this hyperdirect pathway's response has been linked to an inhibition of competing (i.e. incorrect) motor programs (Nambu *et al.*, 2000). For the cortico-thalamic pathway, our model predicts a stronger facilitation of incorrect motor programs in Parkinsonian networks (Fig. 7). This is a behaviorally relevant dysfunction that, to our knowledge, has not been previously described or hypothesised on. Again, we hope to motivate empiricists to investigate if such a dysfunction in fact exists in the brain.

Dopamine replacement (again amounting to 187.5% of pallidal loss) mostly restores pathway outputs on correct and incorrect motor programs towards what we record in healthy networks (Fig. 7): the direct pathway clearly facilitates correct motor programs, the indirect pathway does not detrimentally inhibit them and the cortico-thalamic pathway does not detrimentally facilitate incorrect motor programs. However, medication does not restoratively reduce the hyperdirect pathway's output on incorrect motor programs, but rather strengthens it even further. Again, this argues for a new balance of pathway impacts in medicated Parkinsonian brains.

In the previous subsection, we showed that high dopamine medication results in the development of incorrect 'hyperkinetic' SR associations. Figure 8 depicts the evolution of pathway outputs in these hyperkinetic networks during initial learning, thus addressing detrimental side effects of dopamine medication: none of the four pathways learns to preferentially direct its outputs to either correct or incorrect motor programs. Rather, pathways develop equally strong outputs on correct and incorrect motor programs, thus randomly associating stimuli to responses and showing no sign of adaptation to reward contingencies. At the same time, M1 activity is high, reflecting strong motor output. As expected therefore, high levels of dopamine replacement result in the development of incorrect (i.e. unrewarded) responses, which are typical for dopamine-induced dyskinesias in clinical practice.

Model tests: behavioral outcomes of BG lesions

Lesions of BG nuclei allow us to study network performance with one or more pathways eliminated. The behavioral outcomes of such lesions have been investigated extensively in empirical studies. By simulating lesions of BG nuclei in our neuro-computational model and by comparing the behavioral outcomes of these lesions with empirical findings, we scrutinise the validity of our modeling assumptions. For lesions of striatum, STN, globus pallidus externus (GPe) and GPi, we each ran 100 randomly initialised networks on our three task phases, i.e. initial learning, automatic performance and re-learning (Fig. 9).

Empirically, lesions of dorsal striatum have been shown to slow down initial learning of SR associations in rats, while STN lesions do not have such an effect (Featherstone & McDonald, 2004; El Massioui *et al.*, 2007). Moreover, striatal lesions in cats have been shown to result in impairments in performing a well-learned Go–NoGo task (Aldridge *et al.*, 1997). Our simulations reproduce striatal lesions to impair both learning and automatic performance (Fig. 9, compare first and second row of the first column of

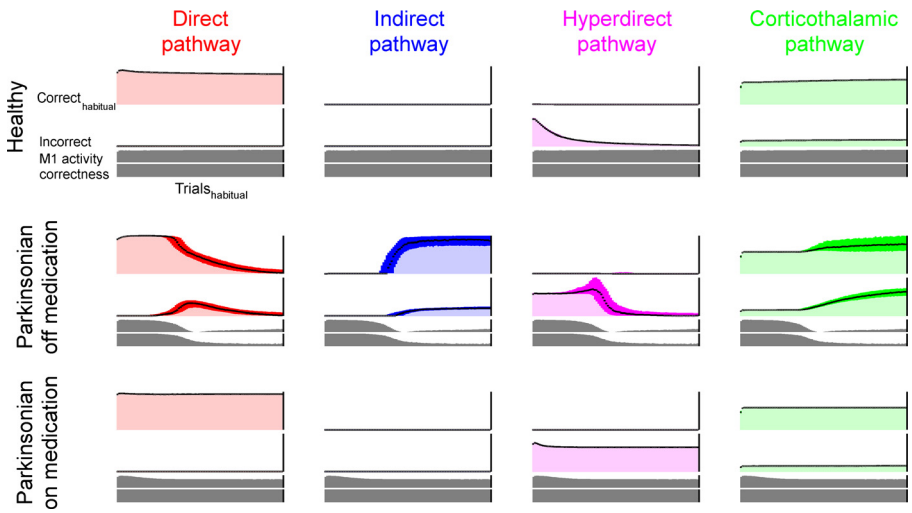

FIG. 7. Pathway outputs on correct and incorrect motor programs in Parkinsonian networks. Subplots depict developments of pathway outputs over the progress of automatic SR performance, separately for the four modeled pathways and for healthy and Parkinsonian networks (the latter on and off medication). Plotted developments start after the initial-learning criterion is reached and continue for 25 000 trials of automatic performance: separate lines within each subplot show the evolution of pathway outputs on correct and incorrect motor programs. For each line, a brightly colored band depicts how lower and upper quartiles of pathway outputs (y axis) evolve over task progress (x axis) – as estimated from 1000 randomly initialised networks; a black line in each band visualises the development of the median. Pathway outputs are defined as average products of synaptic strengths and presynaptic activities, as detailed in 'Materials and methods'. For comparisons, developments of motor-cortical (M1) activities and correct-response rates are rendered below the developments of pathway outputs, where high y values indicate high M1 activity and high correct-response rates, respectively. Pathway outputs were measured every ten trials; dopamine replacement amounts to 187.5% of pallidal dopamine loss. Scalings of the y axes are equivalent for all medical conditions of each pathway, allowing for direct comparisons; comparisons between pathways, however, are not valid because of different scalings.

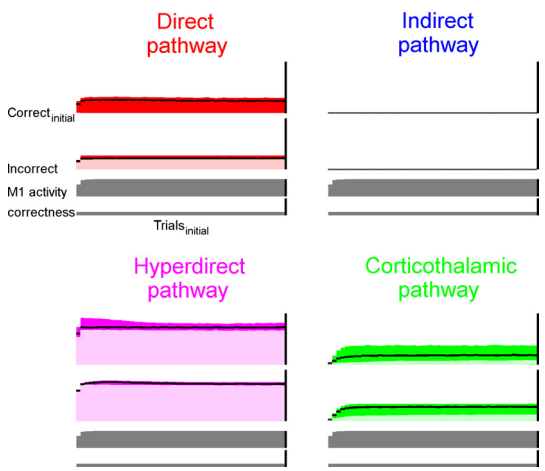

FIG. 8. Development of pathway outputs over the initial-learning period of our task (5000 trials) in Parkinsonian networks that receive a replacement dose amounting to 187.5% of pallidal dopamine loss. Subplots show how the outputs of the four major pathways evolve. Separate lines within each subplot show the evolution of pathway outputs on correct and incorrect motor programs. For each line, a brightly colored band depicts how lower and upper quartiles of pathway outputs (y axis) evolve over task progress (x axis) – as estimated from 1000 randomly initialised networks; a black line in each band visualises the development of the median. Pathway outputs are defined as average products of synaptic strengths and presynaptic activities, as detailed in 'Materials and methods'. For comparisons, developments of motor-cortical (M1) activities and correct-response rates are rendered below the developments of pathway outputs, where high y values indicate high M1 activity and high correct-response rates, respectively. The subplots' y-axes are locked to those in Fig. 4, allowing for direct comparisons; x-axes, however, are not comparable between Figures, as the dopamine-replaced networks shown here were run for 5000 trials (as none of them reached the initial-learning criterion), while networks in Fig. 4 were stopped after reaching the criterion.

subplots); STN lesions are reproduced to not result in any learning impairments. Lesions of dorsal globus pallidus in rats (i.e. the rodent equivalent of GPe) have been empirically shown to specifically disrupt reversal performance in a visual discrimination task, but not acquisition performance and well-learned performance (Evenden *et al.*, 1989). Our simulations reproduce these effects (Fig. 9). Lesions of entopeduncular nucleus in rats (i.e. the rodent equivalent of GPi) have been shown to impair initial-learning and re-learning performances in a reinforcement-based T-maze task (Sarkisov *et al.*, 2003). However, GPi lesions have been reported to result in little or no response-time changes in a well-trained (i.e. automatic) SR task in monkeys (Horak & Anderson, 1984; increases in movement times were, however, reported). In our simulations, we indeed find GPi lesions to severely impair initial-learning and re-learning performances, while automatic performance is spared.

In Parkinsonian humans, both SR learning and habitual performances are severely impaired, even in the absence of any additional lesions of striatum, STN, GPe or GPi (Maddox *et al.*, 2005; Wu & Hallett, 2005). Our simulations reproduce these effects (Fig. 9, compare first and second column of the top row of subplots). For therapeutic reasons, BG lesions have been empirically well explored in PD: GPi pallidotomy (i.e. a lesion of GPi) is still commonly performed in humans suffering from advanced PD. This lesion improves performance in well-learned, everyday movements (Lozano *et al.*, 1995) but impairs feedback-based learning (Sage *et al.*, 2003). To see if our model reproduces these findings, we lesioned GPi in Parkinsonian networks and again investigated learning performances and automatic performance. And indeed, we find GPi pallidotomy to almost perfectly restore automatic performance, while it heavily impairs initial-learning and re-learning performances (Fig. 9; compare top and bottom rows of the second column of subplots). More recently, STN has received attention as a target site for therapeutic lesions as well (Su *et al.*, 2003; Alvarez *et al.*, 2008). In our simulations, however, STN lesions do not significantly influence automatic performance in unmedicated

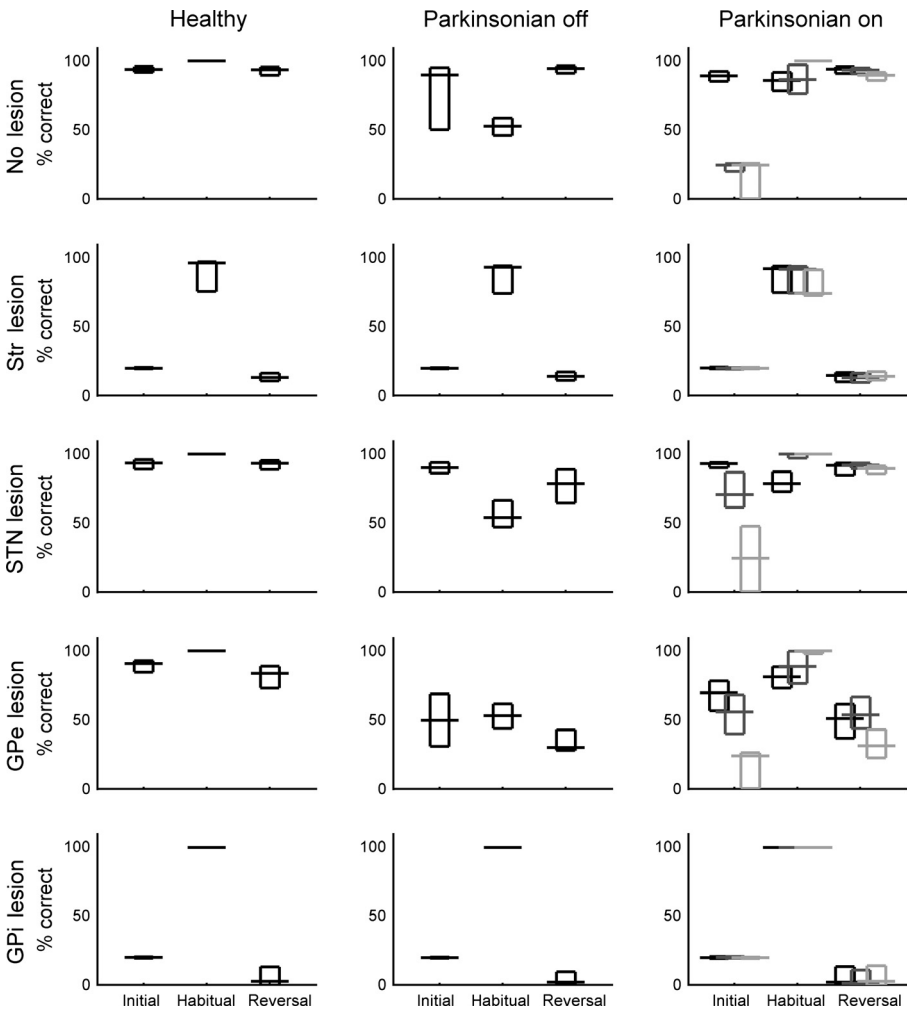

FIG. 9. Behavioral outcomes of focal lesions in BG. Subplots depict initial-learning performance, automatic performance and re-learning performance for unlesioned networks and networks with lesions of striatum, STN, GPe and GPi. Estimated from 100 randomly initialised networks each, bars depict upper quartiles, lower quartiles and medians of correct-response rates. Initial learning and re-learning were evaluated for 2500 trials each, automatic performance for 25 000 trials as detailed in 'Materials and methods'. For medicated Parkinsonian networks, three dopamine doses were evaluated, one chosen relatively low (i.e. as 87.5% of pallidal loss; black bars) such that both learning and automatic performance were suitably alleviated (cf. Fig. 9), one chosen intermediate (i.e. as 125% of pallidal loss; medium gray bars) and the third chosen relatively high (i.e. as 187.5% of pallidal loss; light gray bars) such that automatic performance was fully restored but learning was strongly impaired.

Parkinsonian networks. Thus, our simulations do not reproduce findings of ameliorative effects of STN lesions in unmedicated Parkinsonian monkeys (Bergman *et al.*, 1990). For medicated networks, however, we find that STN lesions do have effects, which depend upon dopamine dosage: with relatively low dopamine doses, STN lesions impair automatic performance, while they improve it with higher doses (Fig. 9; compare first and third row of the third column of subplots). Thus, our simulations suggest that a combination of dopaminergic medication and STN lesions might produce better outcomes than any of these treatments alone. Moreover, we observe that STN lesions produce the smallest impairments in learning performance of all simulated lesion sites. For striatal lesions, we find some improvements in automatic performance. However, we are not aware of any systematic empirical study reporting the effects of striatal lesions in PD. For GPe lesions, we observe impairments in automatic performance in medicated Parkinsonian networks; moreover, GPe lesions cause impairments in learning performances in both medicated and unmedicated Parkinsonian networks. Thus, our simulations agree with findings that GPe is no a good target for therapeutic lesions (Zhang *et al.*, 2006).

Robustness of model performance against parameter changes

To show the robustness of our model against parameter changes, we randomly varied all fixed model parameters of CBGT pathways and re-ran the three phases of our task for a healthy unlesioned model. We randomly drew ten different sets of parameters that differed from the set reported in Tables 1 and 2. Varied parameters included all fixed synaptic weights w, all baseline membrane potentials B (except the baseline of SNc dopamine neurons, which do not belong to CBGT pathways), all error distributions ε, all time constants η and η^{dec}, all threshold parameters γ and all maximum membrane potentials m^{max}. For each set of parameters, we randomly picked each parameter from a uniform distribution with the boundaries $[-10\% + 10\%]$ of the parameter's original value. Values were rounded to achieve a precision of two decimal points (except for time constants which were rounded to nearest integers). Parameters with a value of 0 were left at 0.

We ran 100 networks for each set of parameters and for each of our three task phases. In accordance with the results depicted in Fig. 9, initial learning and re-learning were run for 5000 trials and automatic performance for 25 000 trials.

On average, the networks scored 94.6% correct responses for initial learning (compared with 92.4% for the original set of parameters, as reported in Tables 1 and 2), 99.86% correct responses for automatic performance (compared with 100%) and 95.2% for re-learning (compared with 91.5%). If anything therefore, the varied parameters resulted in better model performance than our reported set, demonstrating the model's independence of particular parameter choices.

Discussion

Via neuro-computational simulations, we showed that dysfunctional synaptic plasticity, as resulting from dopamine loss, can account for the emergence of hypokinetic symptoms in unmedicated PD and hyperkinetic symptoms in medicated PD. In line with previous theories of BG pathway dysfunctions in PD (Albin *et al.*, 1989; DeLong, 1990), we found that dopamine loss results in an average increase in activity of the indirect BG pathway and an average decrease in activity of the direct pathway. However, our simulations suggest that these average changes are not decisive for the emergence of behavioral impairments. They rather predict that, to fully explain how dopamine loss results in motor impairments, pathway outputs that target correct motor programs and those that target incorrect motor programs have to be analysed separately.

Model predictions

Specifically, our simulations predict that the direct pathway facilitates correct motor programs less actively in unmedicated Parkinsonian networks than in healthy networks, while the indirect pathway inhibits these correct motor programs more strongly. This prediction can be investigated empirically: an empiricist may want to record a large number of GPi neurons in the healthy and Parkinsonian brain hemispheres of hemi-Parkinsonian animals while these animals perform a simple SR task. By additionally recording activities from STN and striatum, the empiricist may want to find out which BG pathways trigger particular increases or decreases in GPi firing (cf. Kita & Kita, 2011). According to the prediction, the direct pathway should inhibit GPi neurons less strongly in Parkinsonian than in healthy hemispheres. Moreover, the indirect pathway should excite GPi neurons more strongly, but only those that also receive input from the direct pathway during the same response. Furthermore, our simulations predict that the hyperdirect pathway inhibits *incorrect* motor programs more actively in Parkinsonian networks. Thus, the empiricist should observe that the hyperdirect pathway excites GPi neurons more strongly, but only those that do *not* receive input from the direct pathway during the same response. Thereby, our model predicts that the sets of neurons that are targeted more strongly by indirect vs. hyperdirect pathways in Parkinsonian brains do not overlap. To the best of our knowledge no other model has made such a prediction before.

On a more general level, our simulations predict that PD patients experience increased response conflict when performing SR tasks. This is the case because correct motor programs are facilitated less reliably in Parkinsonian networks and are even actively suppressed. Even if response selection is still reliable enough to produce correct overt responses, neuronal markers of conflict should be observable in brain recordings, like the anterior N2b or the N_E in EEG recordings (cf. Yeung *et al.*, 2004). We recently acquired some evidence for this prediction (Verleger *et al.*, 2013).

As to dopamine replacement, our simulations predict that it results in a new balance of average pathway outputs rather than in restoration of non-Parkinsonian states. In particular, our simulations predict an enhanced average output of the hyperdirect pathway, resulting from a stronger inhibition of incorrect (but not correct) motor programs. Behaviorally, dopamine replacement is predicted to restore well-trained SR performance only when high doses are delivered, while such high doses should cause learning impairments (Fig. 6); low doses, by contrast, are predicted to alleviate learning. To test these predictions, an empiricist could first train animals on an SR task, then lesion their dopamine neurons, administer a high or low dose of levodopa and finally have the animals again perform either the previously learned set of SR associations or an entirely new set.

Comparisons with previous theories and computational models

Our simulations corroborate theories that propose firing-rate changes as causes of motor impairments in PD (e.g. Albin *et al.*, 1989; DeLong, 1990; Nambu, 2005). However, they also suggest that previous theories might require some revisions and extensions. Most importantly, our simulations stress the importance of synaptic plasticity in mediating between dopamine loss and the emergence of behavioral symptoms. While some effects of dopamine loss on synaptic plasticity have been simulated with previous models (e.g. Frank, 2005; Stocco *et al.*, 2010), they have not previously been simulated and analysed in similar detail. Moreover, our simulations highlight the importance of the cortico-thalamic pathway, not included in previous theories of Parkinsonian pathway dysfunctions. A strengthening of synapses in this cortico-thalamic pathway during automatic performance can explain the seemingly paradox findings that lesions of GPi alleviate Parkinsonian symptoms but do not much impair healthy animals' performance in well-trained tasks.

Recently, theories of aberrant oscillatory activity in BG have received much attention (e.g. Engel & Fries, 2010; Jenkinson & Brown, 2011). While these theories have motivated many empirical studies, they are not yet specific about the mechanisms via which dopamine loss results in oscillatory changes and, more importantly, about how oscillatory changes cause motor impairments. Theories of pathway dysfunctions, in contrast (e.g. Mink, 1996; Nambu, 2005), can already well describe causalities between dopamine loss and the emergence of Parkinsonian symptoms.

While there have been previous computational models of dopamine depletion in BG (e.g. Frank *et al.*, 2004; Frank, 2005; Humphries *et al.*, 2006; Guthrie *et al.*, 2009; Stocco *et al.*, 2010; Moustafa & Gluck, 2011), most of these have been used for different aims than our model. Rather than for investigating aberrant connectivity in CBGT pathways in detail, they have been used for reproducing Parkinsonian behavioral dysfunctions (Guthrie *et al.*, 2009; Stocco *et al.*, 2010; Moustafa & Gluck, 2011) or neuronal firing patterns and oscillations (Humphries *et al.*, 2006). Only Frank (2005) put an emphasis on dysfunctions of BG pathways. In his model, bursts in dopamine increase the responses of Go units in the direct pathway and suppress the responses of NoGo units in the indirect pathway, thereby guiding learning of response selection. Dopamine dips result in opposite effects. In PD, phasic increases and decreases in dopamine are reduced according to Frank (2005). This results in a less strong preference for either pathway. Our model, by contrast, predicts that the indirect pathway outweighs the direct pathway in PD. In the 'Model predictions' section, we suggest an empirical test of our model's prediction.

An intriguing prediction of Frank's (2005) model was confirmed by Frank *et al.* (2004): they showed that Parkinsonian patients off medication are better at learning to avoid negative outcomes than at learning to approach positive outcomes, while patients on medication show opposite effects. While Frank *et al.* (2004) and Frank (2005) confined their model to direct and indirect BG pathways, Frank (2006) extended this model to include also the hyperdirect pathway. According to his assumptions, the hyperdirect pathway prevents premature responding in the case of decision conflict. This function differs from the surround-inhibition function predicted by our simulations. However, these functions may not be incompatible.

Frank *et al.* (2007) showed that Frank's (2006) extended model correctly predicts that STN deep brain stimulation (DBS) impairs Parkinson's disease patients in slowing down their responses in situations of high decision conflict. In all of the above-cited studies, Frank and co-workers allowed dopamine-modulated learning only in the striatum and thus pre-specified other connections. By our approach of exploring synaptic plasticity and therefore minimizing pre-wiring of connectivity, we take a new and different perspective.

Limitations

As a limitation of simulation results in general, their validity always depends upon the validity of the underlying model's assumptions. As a plus, however, computational models allow complete insights into their firing rates and synaptic connectivities. Such a complete analysis is not yet possible in the brain because of its enormous number of neurons and synapses. Thus, computational modeling offers a unique tool for performing a fully systemic analysis of Parkinsonian pathophysiology (cf. Bar-Gad & Bergman, 2001).

Our model, moreover, does not allow us to investigate aberrant oscillations in BG. While it is well established that Parkinsonian symptoms are closely linked to an increased power of beta oscillations in BG (Kühn *et al.*, 2006, 2009), the mechanisms via which these oscillations emerge from dopamine loss and via which they produce hypokinesia remain largely unclear. Some computational studies have tried to unveil these mechanisms (van Albada *et al.*, 2009; Holgado *et al.*, 2010; Kumar *et al.*, 2011; McCarthy *et al.*, 2011), but the diversity of their results does not clarify the issues in particular. Thus, we decided against modeling oscillatory activity. To our mind, a simple reproduction of oscillations without establishing a close link to their functions or dysfunctions would not broaden the explanatory scope of our model. Moreover, by excluding potential generators of oscillations (i.e. reciprocal connections between STN and GPe and the extremely complex striatal micro-circuit), we were able to focus on our key question of how the effects of dopamine loss on synaptic plasticity result in imbalances of BG pathways. While more detailed models are always desirable when trying to 're-engineer the brain', they are often less suitable for addressing specific empirical issues. With high levels of detail, moreover, it becomes hard to construct systems-level models that can produce overt behavior. Indeed, the few models that in detail implement the striatal micro-circuit (Tan & Bullock, 2008; Humphries *et al.*, 2009, 2010) do not implement the remaining cortico-BG-thalamic circuit in detail and are not able to produce overt response behavior. We acknowledge that we did not build a full model of BG circuitry because of our decision to not implement the striatal microcircuit, the reciprocal connections between STN and GPe and the connections from GPe to striatum as well as some other minor projections. Inclusion of these fiber tracts would allow for interactions between pathways and might thus result in additional or more complex pathway functions. Additional studies are necessary to investigate such effects.

Moreover, we decided against modeling the effects of DBS. Over the last decade, DBS has become a standard treatment to alleviate Parkinsonian symptoms in humans (Lozano *et al.*, 2002). However, it remains to be clarified how DBS achieves its effects. Tentative evidence suggests that STN DBS might work by silencing STN neurons, thus being vaguely comparable to a lesion of STN (Gradinaru *et al.*, 2009); and indeed, we did simulate STN lesions in our model. However, as long as it remains speculative in how far lesions and DBS differ, we felt uncomfortable trying to simulate the effects of DBS on CBGT pathways.

Finally, we did not model any effects of dopamine on the instantaneous responsiveness of striatal MSNs. Previous computational models of BG (e.g. Frank *et al.*, 2004; Frank, 2005, 2006) assume that dopamine immediately excites striatal D1 MSNs of the direct pathway and inhibits striatal D2 MSNs of the indirect pathway. Indeed, there is empirical evidence pointing towards the existence of immediate dopaminergic effects on striatal ion-channel conductances (Calabresi *et al.*, 1987; Lin *et al.*, 1996; Maurice *et al.*, 2004). It remains to be clarified, however, if dopamine in fact immediately excites the direct and inhibits the indirect pathway (Calabresi *et al.*, 2007). Similarly, it needs to be shown to what extent immediate effects of dopamine on ion-channel conductance fulfill a behaviorally relevant function on their own or to what extent they might in some way support the effects of dopamine on long-term plasticity. As our results and conclusions are focused on the effects of dopamine on synaptic plasticity (and the pathway imbalances resulting from this), we think it a valid assumption to not implement any dopaminergic effects on the instantaneous responsiveness of striatal MSNs.

Conclusion

Our simulations suggest that dysfunctional synaptic plasticity in BG pathways can explain how dopamine loss causes motor impairments. Our simulations predict that synapse-specific changes in BG pathways are more important for determining PD motor impairments than changes in average pathway outputs. Dopamine replacement therapy is predicted to induce a new equilibrium of average pathway outputs and new patterns of connectivity, rather than to simply resurrect non-Parkinsonian connectivity. Our model shows how synaptic plasticity in the cortico-thalamic pathway can resolve puzzling paradoxes associated with the outcomes of stereotaxic GPi lesions. Overall, our model suggests that dysfunctional synaptic plasticity is a major cause of Parkinsonian symptoms, thus calling for a re-conceptualisation of Parkinsonian pathophysiology. It motivates additional computational and empirical research to investigate to what extent dysfunctional synaptic plasticity might interact with immediate effects of dopamine loss on neuronal firing towards the emergence of PD symptoms.

Acknowledgements

H.S. was supported by the German Research Foundation (Deutsche Forschungsgemeinschaft), grants DFG HA2630/7-1 (KFO 247) and DFG HA2630/6-1. In addition, F.H.H. was supported by grant DFG HA2630/4-2. The authors declare no conflict of interests.

Abbreviations

BG, basal ganglia; CBGT, cortico-basalganglio-thalamic; DBS, deep brain stimulation; GPe, globus pallidus external segment; GPi, globus pallidus internal segment; LTD, long-term depression; LTP, long-term potentiation; MSNs medium spiny neurons; PD, Parkinson's disease; SNc, substantia nigra compacta; SR, stimulus–response; STN, subthalamic nucleus.

References

van Albada, S.J., Gray, R.T., Drysdale, P.M. & Robinson, P.A. (2009) Mean-field modeling of the basal ganglia-thalamocortical system. II Dynamics of parkinsonian oscillations. *J. Theor. Biol.*, **257**, 664–688.

Albin, R.L., Young, A.B. & Penney, J.B. (1989) The functional anatomy of basal ganglia disorders. *Trends Neurosci.*, **12**, 166–175.

Aldridge, J.W., Thompson, J.F. & Gilman, S. (1997) Unilateral striatal lesions in the cat disrupt well-learned motor plans in a go/no-go reaching task. *Exp. Brain Res.*, **113**, 379–393.

Alvarez, L., Macias, R., Pavón, N., López, G., Rodríguez-Oroz, M.C., Rodríguez, R., Alvarez, M., Pedroso, I., Teijeiro, J., Fernández, R., Casabona, S., Salazar, S., Maragoto, C., Carballo, M., García, I., Guridi, J., Juncos, J.L., DeLong, M.R. & Obeso, J.A. (2008) Therapeutic efficacy of unilateral subthalamotomy in Parkinson's disease: results in 89 patients followed for up to 36 months. *J. Neurol. Neurosur. Ps.*, **80**, 979–985.

Ashby, F.G., Ennis, J.M. & Spiering, B.J. (2007) A neurobiological theory of automaticity in perceptual categorization. *Psychol. Rev.*, **114**, 632–656.

Bar-Gad, I. & Bergman, H. (2001) Stepping out of the box: information processing in the neural networks of the basal ganglia. *Curr. Opin. Neurobiol.*, **11**, 689–695.

Bayer, H.M. & Glimcher, P.W. (2005) Midbrain dopamine neurons encode a quantitative reward prediction error signal. *Neuron*, **47**, 129–141.

Bergman, H., Wichmann, T. & DeLong, M.R. (1990) Reversal of experimental Parkinsonism by lesions of the subthalamic nucleus. *Science*, **249**, 1436–1438.

Bezard, E., Boraud, T., Bioulac, B. & Gross, C.E. (1999) Involvement of the subthalamic nucleus in glutamatergic compensatory mechanisms. *Eur. J. Neurosci.*, **11**, 2167–2170.

Boyson, S.J., McGonigle, P. & Molinoff, P.B. (1986) Quantitative autoradiographic localization of the D1 and D2 subtypes of dopamine receptors in rat brain. *J. Neurosci.*, **6**, 3177–3188.

Braak, H. & Del Tredici, K. (2008) Cortico-basal ganglia-cortical circuitry in Parkinson's disease reconsidered. *Exp. Neurol.*, **212**, 226–229.

Brown, V.J., Schwarz, U., Bowman, E.M., Fuhr, P., Robinson, D.L. & Hallet, M. (1993) Dopamine dependent reaction time deficits in patients with Parkinson's disease are task specific. *Neuropsychologia*, **31**, 459–469.

Brown, J.W., Bullock, D. & Grossberg, S. (2004) How laminar frontal cortex and basal ganglia circuits interact to control planned and reactive saccades. *Neural Networks*, **17**, 471–510.

Calabresi, P., Mercuri, N., Stanzione, P., Stefani, A. & Bernardi, G. (1987) Intracellular studies on the dopamine-induced firing inhibition of neostriatal neurons *in vitro*: evidence for D1 receptor involvement. *Neuroscience*, **20**, 757–771.

Calabresi, P., Picconi, B., Tozzi, A. & Di Filippo, M. (2007) Dopamine-mediated regulation of corticostriatal synaptic plasticity. *Trends Neurosci.*, **30**, 211–219.

DeLong, M.R. (1990) Primate models of movement disorders of basal ganglia origin. *Trends Neurosci.*, **13**, 281–285.

El Massioui, N., Chéruel, F., Faure, A. & Conde, F. (2007) Learning and memory dissociation in rats with lesions to the subthalamic nucleus or to the dorsal striatum. *Neuroscience*, **147**, 906–918.

Engel, A.K. & Fries, P. (2010) Beta-band oscillations – signalling the status quo? *Curr. Opin. Neurobiol.*, **20**, 156–165.

Evenden, J.L., Marston, H.M., Jones, G.H., Giardini, V., Lenard, L., Everitt, B.J. & Robbins, T.W. (1989) Effects of excitotoxic lesions of the substantia innominata, ventral and dorsal globus pallidus on visual discrimination acquisition, performance and reversal in the rat. *Behav. Brain Res.*, **32**, 129–149.

Featherstone, R.E. & McDonald, R.J. (2004) Dorsal striatum and stimulus–response learning: lesions of the dorsolateral, but not dorsomedial, striatum impair acquisition of a simple discrimination task. *Behav. Brain Res.*, **150**, 15–23.

Frank, M.J. (2005) Dynamic dopamine modulation in the basal ganglia: a neurocomputational account of cognitive deficits in medicated and non-medicated Parkinsonism. *J. Cognitive Neurosci.*, **17**, 51–72.

Frank, M.J. (2006) Hold your horses: a dynamic computational role for the subthalamic nucleus in decision making. *Neural Networks*, **19**, 1120–1136.

Frank, M.J., Seeberger, L.C. & O'Reilly, R.C. (2004) By carrot or by stick: cognitive reinforcement learning in parkinsonism. *Science*, **306**, 1940–1943.

Frank, M.J., Samanta, J., Moustafa, A.A. & Sherman, S.J. (2007) Hold your horses: impulsivity, deep brain stimulation, and medication in parkinsonism. *Science*, **318**, 1309–1312.

Gerfen, C.R., Engber, T.M., Mahan, L.C., Susel, Z., Chase, T.N., Monsma, F.J. & Sibley, D.R. (1990) D1 and D2 dopamine receptor-regulated gene expression of striatonigral and striatopallidal neurons. *Science*, **250**, 1429–1432.

Gradinaru, V., Mogri, M., Thompson, K.R., Henderson, J.M. & Deisseroth, K. (2009) Optical deconstruction of Parkinsonian neural circuitry. *Science*, **324**, 354–359.

Guthrie, M., Myers, C.E. & Gluck, M.A. (2009) A neurocomputational model of tonic and phasic dopamine in action selection: a comparison with cognitive deficits in Parkinson's disease. *Behav. Brain Res.*, **200**, 48–59.

Haber, S.N. (2003) The primate basal ganglia: parallel and integrative networks. *J. Chem. Neuroanat.*, **26**, 317–330.

Holgado, A.J., Terry, J.R. & Bogacz, R. (2010) Conditions for the generation of beta oscillations in the subthalamic nucleus-globus pallidus network. *J. Neurosci.*, **30**, 12340–12352.

Hollerman, J.R. & Schultz, W. (2003) Dopamine neurons report an error in the temporal prediction of reward during learning. *Nat. Neurosci.*, **1**, 304–309.

Horak, F.B. & Anderson, M.E. (1984) Influence of globus pallidus on arm movements in monkeys. I. Effects of kainic acid-induced lesions. *J. Neurophysiol.*, **52**, 290–304.

Humphries, M.D., Stewart, R.D. & Gurney, K.N. (2006) A physiologically plausible model of action selection and oscillatory activity in the basal ganglia. *J. Neurosci.*, **26**, 12921–12942.

Humphries, M.D., Wood, R. & Gurney, K. (2009) Dopamine-modulated dynamic cell assemblies generated by the GABAergic striatal microcircuit. *Neural Networks*, **22**, 1174–1188.

Humphries, M.D., Wood, R. & Gurney, K. (2010) Reconstructing the three-dimensional GABAergic microcircuit of the striatum. *PLoS Comput. Biol.*, **6**, e1001011.

Jahanshahi, M., Wilkinson, L., Gahir, H., Dharminda, A. & Lagnado, D.A. (2010) Medication impairs probabilistic classification learning in Parkinson's disease. *Neuropsychologia*, **48**, 1096–1103.

Jenkinson, N. & Brown, P. (2011) New insights into the relationship between dopamine, beta oscillations and motor function. *Trends Neurosci.*, **34**, 611–618.

Jocham, G., Klein, T.A., Neumann, J., von Cramon, D.Y., Reuter, M. & Ullsperger, M. (2009) Dopamine DRD2 polymorphism alters reversal learning and associated neural activity. *J. Neurosci.*, **29**, 3695–3704.

Kita, H. & Kita, T. (2011) Cortical stimulation evokes abnormal responses in the dopamine-depleted rat basal ganglia. *J. Neurosci.*, **31**, 10311–10322.

Kravitz, A.V., Freeze, B.J., Parker, P.R.L., Kay, K., Thwin, M.T., Deisseroth, K. & Kreitzer, A.C. (2010) Regulation of parkinsonian motor behaviours by optogenetic control of basal ganglia circuitry. *Nature*, **466**, 622–626.

Kühn, A.A., Kupsch, A., Schneider, G.H. & Brown, P. (2006) Reduction in subthalamic 8–35 Hz oscillatory activity correlates with clinical improvement in Parkinson's disease. *Eur. J. Neurosci.*, **23**, 1956–1960.

Kühn, A.A., Tsui, A., Aziz, T., Ray, N., Brücke, C., Kupsch, A., Schneider, G.-H. & Brown, P. (2009) Pathological synchronisation in the subthalamic nucleus of patients with Parkinson's disease relates to both bradykinesia and rigidity. *Exp. Neurol.*, **215**, 380–387.

Kumar, A., Cardanobile, S., Rotter, S. & Aertsen, A. (2011) The role of inhibition in generating and controlling Parkinson's disease oscillations in the basal ganglia. *Front. Syst. Neurosci.*, **5**, 1–14.

Leber, A.B., Turk-Browne, N.B. & Chun, M.M. (2008) Neural predictors of moment-to-moment fluctuations in cognitive flexibility. *Proc. Natl. Acad. Sci. USA*, **105**, 13592–13597.

Lee, B., Groman, S., London, E.D. & Jentsch, J.D. (2007) Dopamine D2/D3 receptors play a specific role in the reversal of a learned visual discrimination in monkeys. *Neuropsychopharmacol.*, **32**, 2125–2134.

Lévesque, M. & Parent, A. (2005) The striatofugal fiber system in primates: a reevaluation of its organization based on single-axon tracing studies. *Proc. Natl. Acad. Sci. USA*, **102**, 11888–11893.

Lin, Y.J., Greif, G.J. & Freedman, J.E. (1996) Permeation and block of dopamine-modulated potassium channels on rat striatal neurons by cesium and barium ions. *J. Neurophysiol.*, **76**, 1413–1422.

Lozano, A.M., Lang, A.E., Galvez-Jimenez, N., Miyasaki, J., Duff, J., Hutchison, W.D. & Dostrovsky, J.O. (1995) Effect of GPi pallidotomy on motor function in Parkinson's disease. *Lancet*, **346**, 1383–1387.

Lozano, A.M., Dostrovsky, J.O., Chen, R. & Ashby, P. (2002) Deep brain stimulation for Parkinson's disease: disrupting the disruption. *Lancet Neurol.*, **1**, 225–231.

Maddox, W.T., Aparicio, P., Marchant, N.L. & Ivry, R.B. (2005) Rule-based category learning is impaired in patients with Parkinson's disease but not in patients with cerebellar disorders. *J. Cognitive Neurosci.*, **17**, 707–723.

Marsden, C.D. & Obeso, J.A. (1994) The functions of the basal ganglia and the paradox of sterotaxic surgery in Parkinson's disease. *Brain*, **117**, 877–897.

Maurice, N., Mercer, J., Chan, C.S., Hernandez-Lopez, S., Held, J., Tkatch, T. & Surmeier, D.J. (2004) D2 dopamine receptor-mediated modulation of voltage-dependent Na^+ channels reduces autonomous activity in striatal cholinergic interneurons. *J. Neurosci.*, **24**, 10289–10301.

McCarthy, M.M., Moore-Kochlacs, C., Gu, X., Boyden, E.S., Han, X. & Kopell, N. (2011) Striatal origin of the pathologic beta oscillations in Parkinson's disease. *Proc. Natl. Acad. Sci. USA*, **108**, 11620–11625.
McHaffie, J.G., Stanford, T.R., Stein, B.E., Coizet, V. & Redgrave, P. (2005) Subcortical loops through the basal ganglia. *Trends Neurosci.*, **28**, 401–407.
Mink, J.W. (1996) The basal ganglia: focused selection and inhibition of competing motor programs. *Prog. Neurobiol.*, **50**, 381–425.
Moore, R.Y. (2003) Organization of midbrain dopamine systems and the pathophysiology of Parkinson's disease. *Parkinsonism Relat. D.*, **9**, 65–71.
Moustafa, A.A. & Gluck, M.A. (2011) A neurocomputational model of dopamine and prefrontal–striatal interactions during multicue category learning by Parkinson patients. *J. Cognitive Neurosci.*, **23**, 151–167.
Nambu, A. (2005) A new approach to understand the pathophysiology of Parkinson's disease. *J. Neurol.*, **252**, IV1–IV4.
Nambu, A., Tokuno, H., Hamada, I., Kita, H., Imanishi, M., Akazawa, T., Ikeuchi, Y. & Hasegawa, N. (2000) Excitatory cortical inputs to pallidal neurons via the subthalamic nucleus in the monkey. *J. Neurophysiol.*, **84**, 289–300.
Nambu, A., Tokuno, H. & Takada, M. (2002) Functional significance of the cortico-subthalamo-pallidal 'hyperdirect' pathway. *Neurosci. Res.*, **43**, 111–117.
Nishibayashi, H., Ogura, M., Kakishita, K., Tanaka, S., Tachibana, Y., Nambu, A., Kita, H. & Itakura, T. (2011) Cortically evoked responses of human pallidal neurons recorded during stereotactic neurosurgery. *Movement Disord.*, **26**, 469–476.
O'Reilly, R.C. & Frank, M.J. (2006) Making working memory work: a computational model of learning in the prefrontal cortex and basal ganglia. *Neural Comput.*, **18**, 283–328.
Parent, A., Lavoie, B., Smith, Y. & Bédard, P. (1990) The dopaminergic nigropallidal projection in primates: distinct cellular origin and relative sparing in MPTP-treated monkeys. *Adv. Neurol.*, **53**, 111–116.
Pavese, N., Rivero-Bosch, M., Lewis, S.J., Whone, A.L. & Brooks, D.J. (2011) Progression of monoaminergic dysfunction in Parkinson's disease: a longitudinal F-dopa PET study. *NeuroImage*, **56**, 1463–1468.
Rascol, O., Brooks, D.J., Korczyn, A.D., De Deyn, P.P., Clarke, C.E. & Lang, A.E. (2000) A five-year study of the incidence of dyskinesia in patients with early Parkinson's disease who were treated with ropinirole or levodopa. *New Engl. J. Med.*, **342**, 1484–1491.
Redgrave, P., Prescott, T.J. & Gurney, K. (1999) The basal ganglia: a vertebrate solution to the selection problem? *Neuroscience*, **89**, 1009–1023.
Sage, J.R., Anagnostaras, S.G., Mitchell, S., Bronstein, J.M., De Salles, A., Masterman, D. & Knowlton, B.J. (2003) Analysis of probabilistic classification learning in patients with Parkinson's disease before and after pallidotomy surgery. *Learn. Memory*, **10**, 226–236.
Sarkisov, G.T., Karapetyan, L.M. & Sarkisyan, Z.S. (2003) The effects of lesioning of the entopeduncular nucleus on the behavior of rats in simultaneous discrimination and open field conditions. *Neurosci. Behav. Physiol.*, **33**, 349–351.
Schroll, H., Vitay, J. & Hamker, F.H. (2012) Working memory and response selection: a computational account of interactions among cortico-basal ganglio-thalamic loops. *Neural Networks*, **26**, 59–74.
Seger, C.A. (2006) The basal ganglia in human learning. *Neuroscientist*, **12**, 285–290.
Shen, W., Flajolet, M., Greengard, P. & Surmeier, J. (2008) Dichotomous dopaminergic control of striatal synaptic plasticity. *Science*, **321**, 848–851.
Smith, Y., Bevan, M.D., Shink, E. & Bolam, J.P. (1998) Microcircuitry of the direct and indirect pathways of the basal ganglia. *Neuroscience*, **86**, 353–387.
Sporer, K.A. (1991) Carbidopa-levodopa overdose. *Am. J. Emerg. Med.*, **9**, 47–48.
Stocco, A., Lebiere, C. & Anderson, J.R. (2010) Conditional routing of information to the cortex: a model of the basal ganglia's role in cognitive coordination. *Psychol. Rev.*, **117**, 541–574.
Su, P.C., Tseng, H.-M., Liu, H.-M., Yen, R.-F. & Liou, H.-H. (2003) Treatment of advanced Parkinson's disease by subthalamotomy: One-year results. *Movement Disord.*, **18**, 531–538.
Tachibana, Y., Kita, H., Chiken, S., Takada, M. & Nambu, A. (2008) Motor cortical control of internal pallidal activity through glutamatergic and GABAergic inputs in awake monkeys. *Eur. J. Neurosci.*, **27**, 238–253.
Tan, C.O. & Bullock, D. (2008) A dopamine–acetylcholine cascade: simulating learned and lesion-induced behavior of striatal cholinergic interneurons. *J. Neurophysiol.*, **100**, 2409–2421.
Verleger, R., Schroll, H. & Hamker, F.H. (2013) The unstable bridge from stimulus processing to correct responding in Parkinson's disease. *Neuropsychologia*, **51**, 2512–2525.
Vitay, J. & Hamker, F.H. (2010) A computational model of the influence of basal ganglia on memory retrieval in rewarded visual memory tasks. *Front. Comput. Neurosci.*, **4**, 13.
Vitek, J.L., Bakay, R.A.E., Freeman, A., Evatt, M., Green, J., McDonald, W., Haber, M., Barnhart, H., Wahlay, N., Triche, S., Mewes, K., Chockkan, V., Zhang, J.-Y. & DeLong, M.R. (2003) Randomized trial of pallidotomy versus medical therapy for Parkinson's disease. *Ann. Neurol.*, **53**, 558–569.
Whone, A.L., Moore, R.Y., Piccini, P.P. & Brooks, D.J. (2003) Plasticity of the nigropallidal pathway in Parkinson's disease. *Ann. Neurol.*, **53**, 206–213.
Wichmann, T. & DeLong, M.R. (1996) Functional and pathophysiological models of the basal ganglia. *Curr. Opin. Neurobiol.*, **6**, 751–758.
Wu, T. & Hallett, M.A. (2005) A functional MRI study of automatic movements in patients with Parkinson's disease. *Brain*, **128**, 2250–2259.
Yeung, N., Botvinick, M.M. & Cohen, J.D. (2004) The neural basis of error detection: conflict monitoring and the error-related negativity. *Psychol. Rev.*, **111**, 931–959.
Zhang, J., Russo, G.S., Mewes, K., Rye, D.B. & Vitek, J.L. (2006) Lesions in monkey globus pallidus externus exacerbate Parkinsonian symptoms. *Exp. Neurol.*, **199**, 446–453.